

# Electronic Properties and Structure of Boron–Hydrogen Complexes in Crystalline Silicon

Joyce Ann T. De Guzman,\* Vladimir P. Markevich, José Coutinho, Nikolay V. Abrosimov, Matthew P. Halsall, and Anthony R. Peaker

The subject of hydrogen–boron interactions in crystalline silicon is revisited with reference to light and elevated temperature-induced degradation (LeTID) in boron-doped solar silicon. Ab initio modeling of structure, binding energy, and electronic properties of complexes incorporating a substitutional boron and one or two hydrogen atoms is performed. From the calculations, it is confirmed that a BH pair is electrically inert. It is found that boron can bind two H atoms. The resulting BH<sub>2</sub> complex is a donor with a transition level estimated at  $E_c - 0.24$  eV. Experimentally, the electrically active defects in n-type Czochralski-grown Si crystals co-doped with phosphorus and boron, into which hydrogen is introduced by different methods, are investigated using junction capacitance techniques. In the deep-level transient spectroscopy (DLTS) spectra of hydrogenated Si:P + B crystals subjected to heat-treatments at 100 °C under reverse bias, an electron emission signal with an activation energy of  $\approx 0.175$  eV is detected. The trap is a donor with electronic properties close to those predicted for boron–dihydrogen. The donor character of BH<sub>2</sub> suggests that it can be a very efficient recombination center of minority carriers in B-doped p-type Si crystals. A sequence of boron–hydrogen reactions, which can be related to the LeTID effect in Si:B is proposed.

Si materials, has been evident in recent research studies.<sup>[1,2]</sup> It has been found that hydrogen enhances the mitigation or deactivation of boron–oxygen defects responsible for the light-induced degradation in Czochralski-grown (Cz) Si solar cells and can passivate detrimental transition metal impurities, dislocation clusters, and thermally induced defects.<sup>[1–5]</sup> On the contrary, it has been suggested that hydrogen is responsible for the so-called light and elevated temperature-induced degradation (LeTID), which can produce a degradation of efficiency of solar cells between 2.5% and 16% relative and is most significant in multicrystalline Si passivated emitter and rear cells (PERC).<sup>[6–9]</sup> In most of the technologically important cases, the details of interaction of hydrogen atoms with other lattice defects are not well understood. It has been speculated that complexes of hydrogen with boron can be involved in some of the aforementioned phenomena.<sup>[9,10]</sup>

## 1. Introduction

The significance of hydrogen in the passivation of recombination active defects and improvement of the efficiency of silicon solar cells, produced from both multicrystalline and monocrystalline

It is known since 1983 that hydrogen passivates boron acceptors.<sup>[11,12]</sup> Although there has been much debate about the mechanism of passivation and structure of the resulting complex, it is now generally accepted that the hydrogen resides at the bond center (BC) between the silicon and the boron; this has strong support from several experimental studies and theoretical calculations.<sup>[13–19]</sup> The common opinion is that the BH pair does not introduce energy levels into the Si bandgap. It has also been suggested that multiple trapping of hydrogen atoms at substitutional boron atoms is possible.<sup>[18,19]</sup>


Early local density functional calculations indicate that atomic hydrogen in B-doped Si binds directly to the boron atom.<sup>[16,17]</sup> They also tell us that at room temperature the H atom effectively roams around all four equivalent Si–B BC sites with a barrier of about 0.2 eV. These calculations already hinted for the removal of the boron shallow acceptor level upon formation of stable BH complexes. Korpás et al.<sup>[18]</sup> showed in their calculations that hydrogen in the form of BH<sub>2</sub> complexes is actually energetically preferred over other known forms of hydrogen in the bulk of B-doped Si, including H<sub>2</sub> molecules.

In view of the importance of the aforementioned findings, they need to be revisited. The calculations were done more than three decades ago, when the size of supercells/clusters hosting the defects was limited to a few tens of atoms, atomistic relaxations were only possible for high symmetry problems (conducted

J. A. T. De Guzman, V. P. Markevich, M. P. Halsall, A. R. Peaker  
Photon Science Institute and Department of Electrical and Electronic Engineering  
The University of Manchester  
Manchester M13 9PL, UK  
E-mail: joyceann.deguzman@manchester.ac.uk

J. Coutinho  
I3N and Department of Physics  
University of Aveiro  
Campus Santiago, 3810-193 Aveiro, Portugal

N. V. Abrosimov  
Leibniz-Institut für Kristallzüchtung (IKZ)  
12489 Berlin, Germany

 The ORCID identification number(s) for the author(s) of this article can be found under <https://doi.org/10.1002/solr.202100459>.

© 2021 The Authors. Solar RRL published by Wiley-VCH GmbH. This is an open access article under the terms of the Creative Commons Attribution License, which permits use, distribution and reproduction in any medium, provided the original work is properly cited.

DOI: 10.1002/solr.202100459

by moving the atoms “manually” as to minimize the electronic energy), and the study of charge states and electronic transitions was still an aspiration among theorists.

Multi-trapping of hydrogen at boron is an old idea which, although postulated previously,<sup>[18,19]</sup> has never been demonstrated experimentally. In addition, the physical mechanisms that could explain a sequential or simultaneous reaction of several hydrogen atoms with boron, as well as the consequences in terms of electrical activity of the resulting complexes, is a problem that is largely unexplored.

Later, we demonstrate that apart from the thermodynamic drive (positive binding energies), and despite having zero net-charge, BH complexes feature a capture radius for atomic hydrogen that is comparable (if not larger) with that of other competing H-traps, including substitutional carbon. The BH<sub>2</sub> complex is predicted to have a donor transition level at  $E_c - 0.24$  eV. With the use of junction capacitance techniques, an effective introduction of an electron trap with an activation energy for electron emission of 0.175 eV has been observed in n-type Cz-Si crystals co-doped with phosphorus and boron. It is argued that this trap is related to the BH<sub>2</sub> complex. A sequence of boron–hydrogen reactions, which can explain the changes in minority carrier lifetime occurring upon LeTID in B-doped p-type Si crystals, is proposed.

## 2. Experimental and Modeling Details

Phosphorus and boron co-doped Si wafers used in the current study were cut from an ingot grown at the Leibniz-Institut für Kristallzüchtung (IKZ) in Berlin by the Czochralski technique. Phosphorus concentration in the wafers was intended to be about  $3 \times 10^{16} \text{ cm}^{-3}$  and boron concentration about  $2 \times 10^{16} \text{ cm}^{-3}$ . To get the required concentrations of phosphorus and boron atoms in the co-doped Si crystal, first, the conditions of growth of Si crystals doped with either phosphorus or boron (one impurity only) were calculated, the test crystals doped with one impurity were grown, and conditions of growth were adjusted to obtain the required amounts and profiles of P and B impurities. After that, the co-doped ingot was grown with growth parameters obtained on the basis of the test growth. Due to the different segregation coefficients of boron and phosphorus in silicon, some changes occur in the [P]/[B] ratio along the ingot. According to our capacitance–voltage measurements, net dopant concentration varied in the range from  $7 \times 10^{15} \text{ cm}^{-3}$  to  $9 \times 10^{15} \text{ cm}^{-3}$  in the bulk regions of the studied samples. Oxygen and carbon concentrations in the wafers have been determined from absorption coefficients,  $\alpha$ , at maxima of infrared absorption bands due to vibrations of interstitial O and substitutional C atoms in silicon.<sup>[20]</sup> The infrared absorption spectra have been recorded at room temperature, and the following values of calibration coefficients for the determination of [O<sub>i</sub>] and [C<sub>s</sub>] have been used:  $[O_i] = 3.14 \times 10^{17} \times \alpha_{O_i} \text{ (cm}^{-3}\text{)}$ ,  $[C_s] = 0.94 \times 10^{17} \times \alpha_{C_s} \text{ (cm}^{-3}\text{)}$ .<sup>[20]</sup> Oxygen concentration is found to be  $(6.5 \pm 0.5) \times 10^{17} \text{ cm}^{-3}$  and carbon concentration to be  $(4.5 \pm 1) \times 10^{16} \text{ cm}^{-3}$  in the Cz-Si:P + B wafers. For a comparison to assess the role of carbon, a few wafers from a Czochralski-grown ingot doped with phosphorus and intentionally enriched with carbon during growth have been studied. Concentrations of impurities in the

Cz-Si:P + C wafers were as follows:  $[P] = (1.0\text{--}1.5) \times 10^{15} \text{ cm}^{-3}$ ,  $[O_i] = (7.5 \pm 0.5) \times 10^{17} \text{ cm}^{-3}$ , and  $[C_s] = (4.0 \pm 0.5) \times 10^{17} \text{ cm}^{-3}$ .

As-received wafers were chemomechanically polished with the thickness of about 450  $\mu\text{m}$ . Prior to hydrogenation processing, the wafers were cleaned using trichloroethylene, acetone, and methanol for 5 min at each step and lightly etched in a solution of hydrofluoric and nitric acids with a 1HF:7HNO<sub>3</sub> ratio. Hydrogen was introduced into the samples either by wet chemical etching at room temperature using the 1HF:7HNO<sub>3</sub> solution or by a treatment in remote hydrogen plasma at room temperature. The parameters of the plasma used are as follows: RF power has been 50 W with 1–2 mBar chamber pressure and 200–250  $\text{cc min}^{-1}$  gas flow.

For the investigation of electrically active defects in the hydrogenated wafers, Schottky barrier diodes (SBDs) were fabricated on samples cut from the wafers. The SBDs on the hydrogenated Cz-Si samples were prepared by thermal evaporation of gold through a shadow mask. Subsequently, aluminum was deposited at the back of the sample to serve as an Ohmic contact. The diode area for all the samples is about 0.79  $\text{mm}^2$  with a recorded leakage current of <0.1 mA at 10 V reverse bias.

We have conducted current–voltage and capacitance–voltage (C–V) measurements with 1 MHz probing voltage signal to assess the quality of the fabricated diodes and to determine the concentration of uncompensated donors,  $N_d^+ = N_{D(\text{total})} - N_A^-$  (where  $N_{D(\text{total})}$  is the total concentration of donors with energy levels in the upper half of the bandgap and  $N_A^-$  is the concentration of compensating acceptor centers),<sup>[21]</sup> as well as the width of the depletion regions. Deep-level transient spectroscopy (DLTS) and Laplace DLTS (L-DLTS) were used to detect and characterize deep-level traps.<sup>[21,22]</sup>

Total energy calculations were conducted from first-principles, within hybrid density functional theory. We used the range-separated functional of Heyd, Scuseria, and Ernzerhof (HSE06),<sup>[23,24]</sup> as implemented by the Vienna Ab initio Simulation Package (VASP).<sup>[25,26]</sup> The projector-augmented wave method was used to treat the core electrons,<sup>[27]</sup> whereas valence states were expanded in plane waves with a cutoff energy of 400 eV. The latter were found self-consistently by energy minimization, leading to a numerical accuracy of the total energy of  $10^{-7}$  eV (as found from the energy change between the last two self-consistent steps).

Defects were inserted in 216- and 512-atom supercells with cubic shape, constructed by replication of  $3 \times 3 \times 3$  and  $4 \times 4 \times 4$  conventional cells of silicon. The calculated lattice constant was  $a = 5.4318 \text{ \AA}$ . Forces acting on atomic nuclei were obtained within the generalized gradient approximation (GGA) to the exchange correlation potential.<sup>[28]</sup>

Minimum energy structures were found by energy minimization with respect to the atomic coordinates, until the maximum residual force was lower than  $0.01 \text{ eV \AA}^{-1}$ . For the calculation of forces and structural relaxation of defects in 216- and 512-atom cells, the band structure was sampled over a  $2 \times 2 \times 2$  k-point grid and  $\Gamma$ -point, respectively. For total energy calculations (HSE06-level), the sampling was done at the  $\Gamma$ -point, irrespective of the cell size. All total energies of defects with nonzero charge include a periodic charge correction, calculated here according to the recipe of Freysoldt et al.<sup>[29]</sup>

### 3. Modeling Results

#### 3.1. Calculated Structures, Transition Levels, and Binding Energies

We have inspected several configurations of BH and BH<sub>2</sub> complexes and found that in p-type Si, the formation of direct B–H bonds notably leads to the most stable structures. **Figure 1** shows the lowest energy configurations of the BH and BH<sub>2</sub> complexes. These are in agreement with previous results in the literature.<sup>[16–18]</sup>

Metastable BH structures where H sits at antibonding sites connected to the B atom, or to its Si first neighbor,<sup>[16]</sup> were found to be less stable than the ground state structure by at least 1.3 eV. On the contrary, the total energy of the BH complex where H is located at the second-neighbor BC site closest to boron was only 0.3 eV above the ground state (first-neighbor BC site). The barrier for the capture of positively charged hydrogen by negatively charged boron, where H<sup>+</sup> performs a jump from the second- to first-neighbor BC site, was estimated as 0.68 eV. This barrier is nearly 0.2 eV higher than the activation energy for migration of H<sup>+</sup>, but still low enough to allow the reaction H<sup>+</sup> + B<sub>s</sub><sup>−</sup> → BH<sup>0</sup> to take place at room temperature.

While the supercell with the most stable BH complex displays a clean bandgap, the neutral BH<sub>2</sub> defect shown in Figure 1 has a semioccupied Kohn–Sham state edging the conduction band minimum, suggesting a donor character. Electronic transition levels  $E(q/q')$  between charge states  $q$  and  $q'$  were evaluated according to the usual expression

$$E(q/q') = \frac{E(q) - E(q')}{q' - q} \quad (1)$$

where  $E(q)$  is the total energy of a supercell with a defect in charge state  $q$ . This already includes a periodic charge correction (about 0.10 and 0.03 eV for BH defects with charge  $q = +1$  in 216- and 512-atom cells, respectively).

We confirm that the BH complex is electrically inert. The defect consists of a B<sup>−</sup>H<sup>+</sup> donor–acceptor pair, where the negatively charged boron atom raises the emptied donor state of hydrogen above the conduction band minimum. Therefore, donor and acceptor transitions of BH are resonant with the valence band and conduction band, respectively.

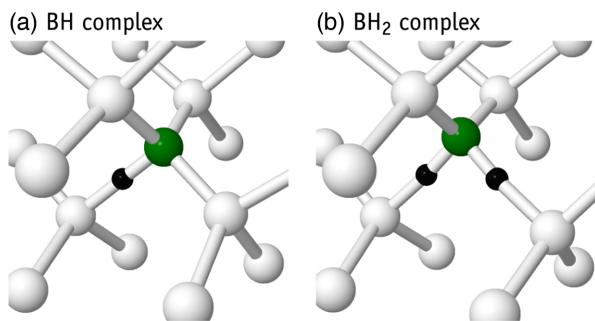
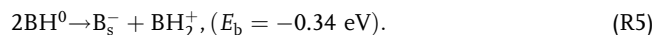
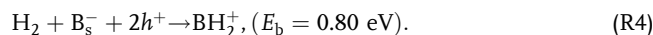
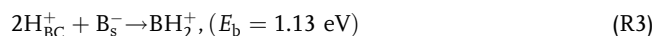
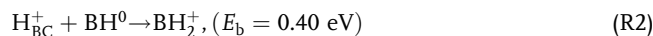
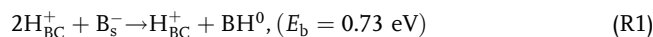


**Figure 1.** Atomistic models of a) BH and b) BH<sub>2</sub> complexes in silicon. Si, B, and H atoms are shown in white, green, and black, respectively.

Regarding BH<sub>2</sub>, we calculated a transition at  $E(0/+)-E_v = 0.91$  eV. The energy of the valence band top,  $E_v$ , was obtained from the energy of the highest occupied Kohn–Sham state of a bulk cell at  $\mathbf{k} = \Gamma$ . The donor level can be cast with respect to the conduction band minimum as  $E_c - E(0/+) = 0.24$  eV, where  $E_g = E_c - E_v = 1.15$  eV is the calculated bandgap width. The BH<sub>2</sub>(0/+) level almost coincides with that obtained for interstitial hydrogen at the BC site, i.e., at  $E_c - E(0/+) = 0.22$  eV. The error bars of the calculated transition energies of both defects are comparable.

The energy balance of reactions between H and B was also investigated. Previous publications disregarded charge state effects,<sup>[16–19]</sup> despite several reactants being charged in p-type silicon. We assume that in B-doped Si the boron is ionized and that any dissolved atomic hydrogen is positively charged at BC sites (H<sub>BC</sub><sup>+</sup>). We also consider the possibility of reactions between boron and molecular hydrogen. Accordingly, the following binding energies,  $E_b$ , could be estimated



In the aforementioned reactions, positive (negative) values of  $E_b$  stand for exothermic (endothermic) processes. Clearly, from the perspective of energetics, sequential capture of at least two protons by boron is a favorable process (Reaction (R1)–(R3)). Also, favorable is the capture of molecular hydrogen by a boron dopant when free holes are available (Reaction (R4)). This is unlikely to take place in an n-type material. Finally, Reaction (R5) tells us that the transfer of a proton between two BH complexes is an endothermic process. Therefore, our results suggest that the capture of hydrogen by boron in crystalline silicon is energetically favored either when H is available in the form of interstitial protons or molecules. However, if the boron concentration exceeds that of hydrogen, energetics favors a distribution of H in the form of boron monohydrides (as opposed to BH<sub>2</sub> complexes).

The net result of any of the aforementioned reaction paths leading to the formation of BH<sub>2</sub> is the consumption of an acceptor (boron) to form a donor (BH<sub>2</sub>). The consequence of this is that CV measurements will show an increase in two uncompensated donors ( $N_d^+$ ) for each BH<sub>2</sub> center formed.

#### 3.2. Analysis of the Effective Radius for the Capture of Hydrogen by Impurities

Despite the calculated positive binding energies involving boron–hydrogen reactions, other traps compete for hydrogen in the silicon. In solar-grade material, among the most common traps in the bulk, we usually find substitutional carbon and interstitial oxygen impurities. While OH defects dissociate at about room temperature,<sup>[30]</sup> carbon–hydrogen complexes are stable up to

100 °C in darkness.<sup>[31–33]</sup> It is therefore important to understand how likely is the formation of BH<sub>2</sub>, in particular via Reaction (R2), in the presence of carbon in the silicon. For that, we estimated how large can be the radii for the capture of a proton by substitutional carbon, substitutional boron, and BH defects.

We considered three types of long-range attractive fields which contribute for the capture of H<sup>+</sup><sub>BC</sub>. The first comes from strain cancellation. This is conveniently described by the elastic energy  $E_{\text{elast}} = P_{ij}^{(a)} G_{ijkl} P_{kl}^{(b)}$  involving two defects separated by  $\mathbf{r} = \mathbf{r}^{(b)} - \mathbf{r}^{(a)}$ , whose elastic dipoles tensors  $P^{(a)}$  and  $P^{(b)}$  interact through an elastic medium with second derivatives of the elasticity Green's function  $G_{ijkl} = \partial^2 G_{ik} / \partial x_j \partial x_l$ .<sup>[34,35]</sup> The derivatives are with respect to the coordinates of the vector distance  $\mathbf{r}$  and  $G_{ik}$  is here approximated to the case of an isotropic material (which has an analytical form)

$$G_{ik}(\mathbf{r}) = \frac{1}{16\pi\mu(1-\nu)} \left[ (3-4\nu)\delta_{ik} + \frac{x_i x_k}{r^2} \right] \frac{1}{r} \quad (2)$$

were the shear modulus  $\mu = 65.5$  GPa and Poisson ratio  $\nu = 0.22$  of silicon were found according to Voight's averaging.<sup>[36]</sup> We can write the elastic energy as  $E_{\text{elast}} = A/r^3$ , where  $A$  represents an "elastic interaction strength" that depends on the relative orientation of the two defects and on the orientation of  $\mathbf{r}$ . Further details for the calculation of  $G_{ijkl}$  and the elastic dipole tensor elements can be found in previous studies.<sup>[35,37]</sup>

We inspected the magnitude of the values that  $A$  typically has when considering the interaction between H<sup>+</sup><sub>BC</sub> and either C<sub>s</sub>, B<sub>s</sub><sup>−</sup>, or BH<sup>0</sup> defects. For the case of substitutional carbon and boron we found strong interaction strengths, respectively  $A = -14.6$  and  $-10.5$  eVÅ<sup>3</sup>, when H<sup>+</sup><sub>BC</sub> is located and aligned along  $\langle 111 \rangle$  directions with respect to the impurity. This results from the superposition of tensile and compressive stress fields from the substitutional impurities and hydrogen. Conversely, when  $\mathbf{r}$  is parallel or nearly parallel to  $\langle 100 \rangle$  directions,  $A \approx 0$  because the strain field of H along those directions is rather weak.

The B–H bond in the BH complex is aligned along one of the  $\langle 111 \rangle$  crystalline directions. Maximum attraction for a remote H<sup>+</sup><sub>BC</sub> is found when the proton is located at regions perpendicular to the B–H bond. The elastic strength is in the range  $A = -11.5$  and  $-5.5$  eVÅ<sup>3</sup> for  $\mathbf{r}$  along  $\langle \bar{1} \bar{1} 2 \rangle$  and  $\langle 1 \bar{1} 0 \rangle$ . In both cases, the alignment of the Si–H<sup>+</sup>–Si compressive unit is nearly perpendicular to the BH axis as to result in a strain cancellation effect. When H<sup>+</sup><sub>BC</sub> is located along the BH axis, a negligible value of  $A$  is obtained. This is due to a minute elastic dipole component along the symmetry axis of BH.

The second type of interactions is the Coulomb attraction between charged defects. This is important to describe the reaction between B<sub>s</sub><sup>−</sup> and H<sup>+</sup><sub>BC</sub> defects, and it is simply given by  $E_{\text{chg-chg}} = e^2/4\pi\epsilon r$ , where  $\epsilon$  is the dielectric constant of silicon. Finally, the third type of interactions considered are those involving an electric dipole and a monopole. This is expected to be important to describe the long-range potential energy of BH (which has a permanent dipole moment) and H<sup>+</sup><sub>BC</sub>. Accordingly

$$E_{\text{dipol-chg}} = \frac{e}{4\pi\epsilon r^2} p \cos \theta \quad (3)$$

where the angle  $\theta$  stands for the misalignment between the BH electric dipole  $\mathbf{p}$  and the vector distance  $\mathbf{r}$  to the H<sup>+</sup><sub>BC</sub> defect. Note that although not having the reach of the Coulomb monopole–monopole field, the  $r^{-2}$  decay of the dipole–monopole energy is substantially more gentle than that of the strain interactions.

The electric dipole moment of the BH defect was calculated from first principles using the double-inverted-cell method<sup>[38]</sup> combined with the expression for the energy of an infinite array of dipoles arranged in a cubic lattice with characteristic spacing  $L$ ,<sup>[39]</sup>  $E_{\text{dipol},\infty} = -p^2/24\pi\epsilon L^3$ . We find that  $p = 6.96D = 1.45$  eÅ, which is coherent with the B–H bond length obtained from the first-principles calculations ( $r_{\text{BH}} = 1.34$  Å), i.e., close to  $p = er_{\text{BH}} = 1.34$  eÅ for a simple point-charge dipole model.

The capture radius ( $r_c$ ) of a defect trap for hydrogen is defined as the trap-H distance below which the H atom is not able to thermally escape from the attractive field of the trap. Therefore

$$k_B T < \frac{e}{4\pi\epsilon} \left( \frac{e}{r_c} + \frac{p \cos \theta}{r_c^2} \right) - \frac{A}{r_c^3} \quad (4)$$

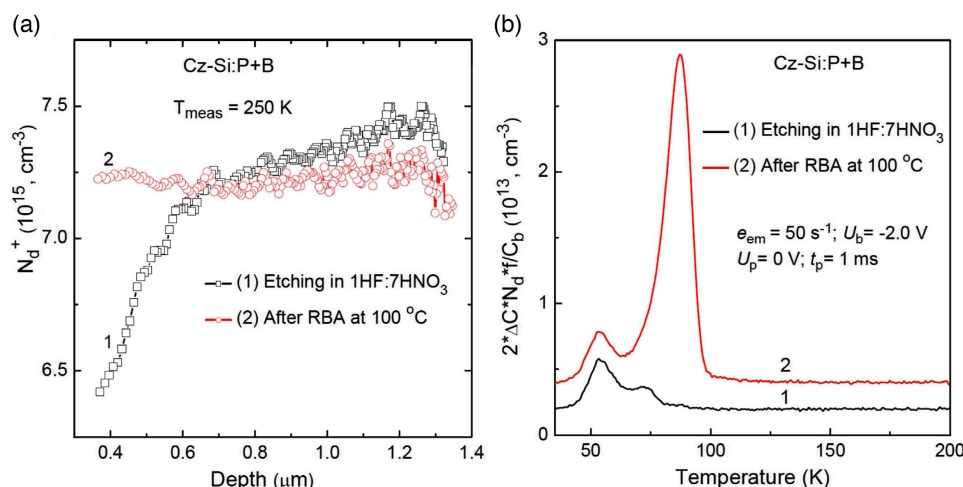
where the three terms on the right are ordered by their range of action. For simple tetrahedral carbon and boron impurities, we obtain respectively  $r_c = 8.3$  Å and  $r_c = 50$  Å at room temperature, clearly showing a far greater trapping efficiency of the boron ion, despite the stronger tensile strain field of the carbon impurity.

For the capture of hydrogen by BH, we note that its tensile field dominates the attraction of hydrogen when  $\mathbf{r}$  is perpendicular to the B–H bond, whereas the electric dipole field is the most influential attraction force along the BH axis. From Equation (4), we find  $r_{c,\perp} = 7.4$  Å and  $r_{c,\parallel} = 8.8$  Å, where subscripted  $\perp$  and  $\parallel$  symbols stand for interactions perpendicular and along the bond of the BH complex. We note that the B–H bond can reorient quite easily (even below room temperature), thus allowing the defect to align itself as to minimize the energy of the H<sup>+</sup>B<sup>−</sup> · · · H<sup>+</sup> structure with respect to both the electrostatic and elastic interactions. Therefore, and despite being a neutral defect, the BH complex shows a capture radius for H<sup>+</sup><sub>BC</sub> that is comparable with, if not larger than, that of substitutional carbon.

## 4. Experimental Results

Figure 2a shows spatial profiles of uncompensated donors ( $N_d^+$ ) in a diode on a hydrogenated Si:P + B sample in an as-hydrogenated state and after annealing at 100 °C for 20 min under reverse bias of  $U_b = -9$  V. A decrease in the  $N_d^+$  values in the region from 0.4 to 0.8 μm in the as-hydrogenated diode is related to passivation of phosphorus donors by negatively charged hydrogen atoms, which were introduced into the bulk regions by wet chemical etching.<sup>[32,40]</sup> It is known that P–H pairs are not very stable and dissociate upon annealing at temperatures around 100 °C.<sup>[40,41]</sup> Indeed, after annealing of the sample at 100 °C for 20 min a recovery of the  $N_d^+$  values in the subsurface region occurred. We have conducted this annealing with the reverse bias of  $U_b = -9$  V applied to the diode (reverse bias annealing, which is referred to as RBA in the following). The reason for the application of the reverse bias was to transform

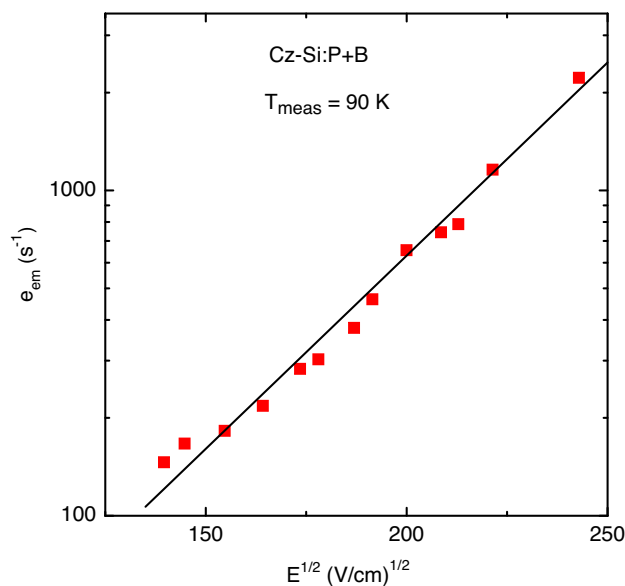




**Figure 2.** a) Spatial profiles of concentration of uncompensated shallow donors measured at 250 K in a diode on Cz-Si:P + B sample, which was subjected to the following subsequent treatments: (1) Etching in 1HF:7HNO<sub>3</sub> solution at room temperature for 3 min; (2) annealing at 100 °C for 20 min during which a reverse bias of  $U_b = -9$  V was applied. b) DLTS spectra recorded for a diode,  $N_d^+(W)$  dependencies of which are shown in (a). The spectra are shifted along the vertical axis for clarity. Measurement parameters are given in the graph.

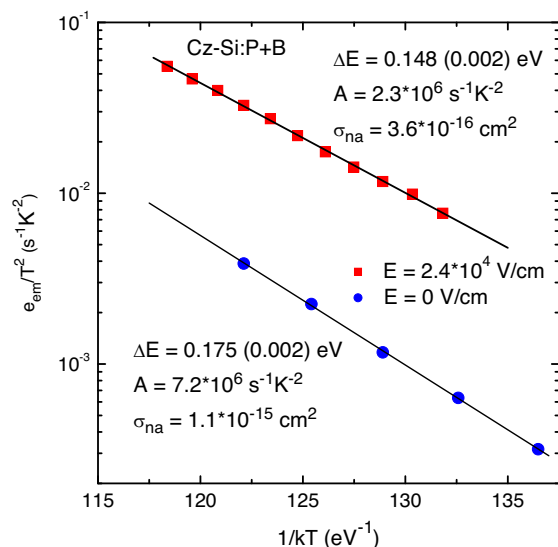
hydrogen atoms from the negatively charged state to the positive one in the space charge region of the reverse-biased diodes. This initiates interactions of  $H^+$  species with negatively charged boron atoms.

Figure 2b shows conventional DLTS spectra for a diode,  $N_d^+(W)$  dependencies of which are shown in Figure 2a. The spectra are representative of a region from about 0.35 to 0.7  $\mu\text{m}$  from the surface. Concentration values  $Y = 2 \times (\Delta C/C_b) \times N_d \times f$  are shown in Figure 2b, where  $\Delta C$  is the magnitude of a capacitance transient,  $C_b$  is the bias capacitance, and  $f$  is the correction function, which takes into account depletion widths at the bias and pulse voltages and the so-called “lambda” layer.<sup>[21]</sup> The  $Y$  values at the peak maxima are close to the average trap concentrations in the probed region. Two relatively weak electron emission related peaks with their maxima at about 55 and 73 K are observed in the spectrum recorded just after the hydrogenation. These peaks can be related to oxygen-related thermal double donors, carbon-hydrogen, and carbon-oxygen-hydrogen complexes.<sup>[32,33,41–44]</sup> Annealing at 100 °C under reverse bias has resulted in the appearance of a strong electron emission signal with its maximum at about 87 K in the DLTS spectrum. It can be seen from Figure 2b that the average concentration of the RBA-induced trap is about  $2.5 \times 10^{13} \text{ cm}^{-3}$ . It has been found that the detected electron trap has a very strong dependence of electron emission rate,  $e_{\text{em}}$ , on electric field ( $E$ ) in the space charge region of the diodes, which is a characteristic for the Poole–Frenkel mechanism ( $e_{\text{em}} \approx \exp\sqrt{E}$ ),<sup>[21,45]</sup> as shown in Figure 3. This finding indicates a donor character of the trap. Figure 4 shows an Arrhenius plot of electron emission rates for the donor trap, which have been measured with the use of L-DLTS at the average electric field of  $E \approx 2.4 \times 10^4 \text{ V cm}^{-1}$ . This dependence is compared with that for the  $e_{\text{em}}$  values at  $E = 0 \text{ V cm}^{-1}$ . The  $E$ -zero-field  $e_{\text{em}}$  values have been obtained from fitting the experimental  $e_{\text{em}}(E)$  dependencies according to the Hartke’s 3D extension of the standard Poole–Frenkel model.<sup>[45]</sup> The activation energy of electron emission



**Figure 3.** Dependence of electron emission rate on electric field in depletion region of a diode on Cz-Si:P + B sample, which was subjected to annealing at 100 °C for 20 min with the reverse bias of  $U_b = -9$  V applied. Hydrogen was introduced into the sample by etching in 1HF:7HNO<sub>3</sub> solution at room temperature for 3 min. Measurements were conducted at 90 K using double L-DLTS technique with the reverse bias fixed at  $U_b = -9$  V and changeable values of voltage for both filling pulses with the difference of 0.5 V between them.

from the corresponding energy level at zero electric field has been determined as 0.175 eV relative to conduction band edge (Figure 4). In the following the donor trap detected will be referred to as the  $E_{0.175}$  trap. It should be mentioned that the obtained value of the activation energy of electron emission for the  $E_{0.175}$  trap coincides with that for the  $E3'$  trap, which has been assigned to the bond-centered hydrogen atom in Si.<sup>[30]</sup>



**Figure 4.** Arrhenius plots of  $T^2$ -normalized electron emission rates recorded in the temperature range 85–100 K at different values of electric field on diodes on Cz-Si:P+B samples, which were subjected to hydrogenation and annealing at 100 °C for 20 min during which a reverse bias of  $U_b = -9$  V was applied. The emission rates at the average electric field of  $E \approx 2.4 \times 10^4$  V cm $^{-1}$  have been obtained from measurements with the use of L-DLTS technique with the reverse bias fixed at  $U_b = -0.5$  V and  $U_p = 0$  V. The emission rates at  $E = 0$  V cm $^{-1}$  have been obtained from fitting the experimental  $e_{em}(E)$  dependencies according to the 3D Hartke model.<sup>[45]</sup> The  $e_{em}(E)$  measurements have been conducted using double L-DLTS technique with the reverse bias fixed at  $U_b = -5$  V and changeable values of voltage for both filling pulses with the difference of 0.2 V between them.

The appearance of donor centers upon reverse bias annealing of CZ-Si:P+B samples with SBDs can be clearly seen in the samples into which more hydrogen has been introduced with the use of hydrogen plasma treatments. The techniques of hydrogenation of silicon samples were discussed in the study by Sopori et al.,<sup>[46]</sup> where it was noted that the amount of hydrogen which could be introduced into silicon samples by H plasma treatments with sufficiently long duration (a few tens of minutes, as in our case) is very much greater than that introduced by wet chemical etching. **Figure 5a** shows spatial profiles of uncompensated shallow donors in a diode on a plasma-hydrogenated Si:P+B sample in as-hydrogenated state and after annealing at 100 °C for 20 min under reverse bias of  $U_b = -9$  V. The treatment at 100 °C under reverse bias has resulted in the significant increase in concentration of uncompensated shallow donors ( $\Delta N_d^+ > 2 \times 10^{15}$  cm $^{-3}$ ) in the subsurface region of the diode ( $W < 0.3$   $\mu$ m) with respect to the bulk  $N_d^+$  value. **Figure 5b** shows conventional DLTS spectra for a diode,  $N_d^+(W)$  dependencies of which are shown in **Figure 5a**. The RBA treatment has resulted in the appearance of a very strong electron emission signal, the electronic signatures (emission activation energy, preexponential factor, and electric-field enhancement of emission) of which are identical to those for the  $E_{0.175}$  donor trap detected in SBDs on samples with hydrogen introduced by wet chemical etching. In the RBA-treated sample the DLTS spectrum represents electron emission in a region from about 0.2 to about 0.6  $\mu$ m from the surface.

A comparison of magnitudes of the peak with its maximum at 87 K in the DLTS spectra shown in **Figure 2b** and **5b** shows that the average concentration of the RBA-induced donor traps in the plasma-hydrogenated samples ( $N_{E_{0.175}} \approx 3 \times 10^{14}$  cm $^{-3}$ ) exceed that in the wet chemically etched samples ( $N_{E_{0.175}} \approx 2.5 \times 10^{13}$  cm $^{-3}$ ) by more than one order of magnitude. The obtained concentration ratio is consistent with the higher amount of hydrogen introduced into the samples by the H-plasma treatment compared with wet etching.

**Figure 6** shows concentration profile of the  $E_{0.175}$  donor trap in a plasma-hydrogenated sample which was subjected to the RBA treatment. Concentration of the deep donor nearly reaches the  $10^{15}$  cm $^{-3}$  value at 0.2  $\mu$ m distance from the surface and decreases to a negligible value at  $W \geq 0.7$   $\mu$ m. A comparison of the concentration profiles in **Figure 5a** and **6** shows that increase in the  $N_d^+$  values in the subsurface region of the RBA-treated diode follows twice the magnitude of the concentration profile of the  $E_{0.175}$  donor trap. As discussed previously this is expected as the creation of each  $E_{0.175}$  donor consumes a boron acceptor and so the change in the  $N_d^+$  values will correspond to twice the trap concentration at each point on the profile.

It is found that the donor defects induced by reverse bias annealing disappear when the RBA-treated samples are kept at temperatures above 280 K with no bias applied to the diodes. On the contrary, these defects are stable up to 400 K in the depletion region of the diodes, i.e., when the diodes are heated up with the reverse bias applied. Apparently, the annihilation of the donor centers is facilitated by the availability of free electrons. **Figure 7** shows changes in the  $N_d^+(W)$  dependencies in a diode on Cz-Si:P+B sample, which was subjected to the following subsequent treatments: 1) hydrogenation in H plasma at room temperature for 30 min; 2) annealing at 100 °C for 20 min with applied reverse bias of  $U_b = -9$  V; and 3) storage at 290 K under open-circuit conditions. The storage at 290 K results in a gradual decrease in the  $N_d^+$  values in the region from 0.3 to 1.0  $\mu$ m from the surface. The decrease can be described by a monoexponential decay process as it is evidenced in **Figure 8**. **Figure 8** shows a decay of the average  $N_d^+(W)$  values in the region from 0.4 to 0.5  $\mu$ m from the surface for the diode, the  $N_d^+(W)$  dependencies of which are shown in **Figure 7**, upon keeping it at 290 K under open-circuit conditions. The decay rate is found to be about  $1.9 \times 10^4$  s $^{-1}$  at 290 K. It should be noted that the  $N_d^+(W)$  values in region from 0.3 to 1.0  $\mu$ m from the surface, which were measured after relatively long storage of the RBA-treated sample at room temperature, differ from the values in the as-hydrogenated state as a comparison of curves 1 and 6 in **Figure 7** shows, i.e., the  $N_d^+(W)$  values are not fully recovered after a cycle of RBA and open-circuit storage treatments.

It is further found that the storage of the hydrogenated and RBA-treated sample at 290 K under open-circuit conditions results in a gradual decrease in the magnitude of the DLTS peak with its maximum at 87 K (**Figure 9**). The time constants of the processes, which result in the changes in the  $N_d^+(W)$  values and the DLTS peak magnitude due to the  $E_{0.175}$  trap upon storage of the diode at 290 K, are very close. This observation further confirms that the observed changes in the  $N_d^+(W)$  values are related to the changes in concentration of the  $E_{0.175}$  donor trap.

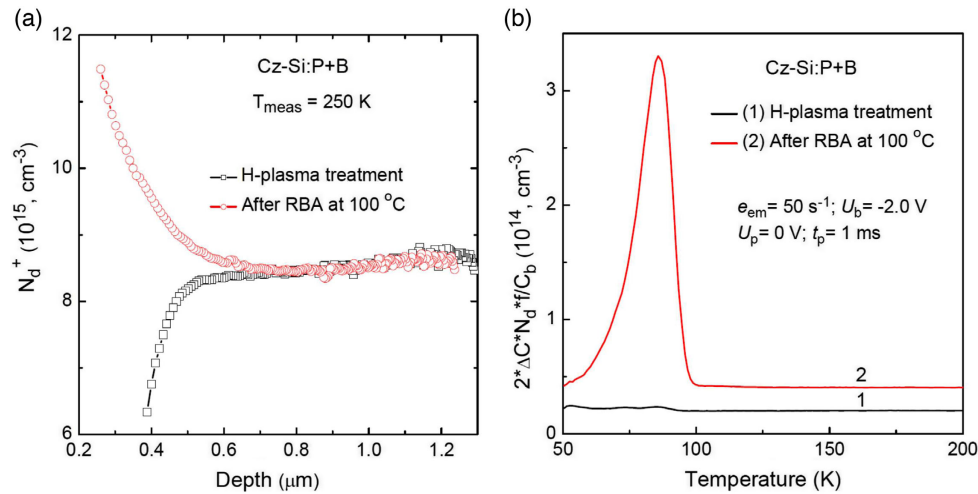


**Figure 5.** a) Spatial profiles of concentration of uncompensated shallow donors measured at 250 K in a diode on Cz-Si:P + B sample, which was subjected to the following subsequent treatments: 1) hydrogenation in H plasma at room temperature for 30 min; 2) annealing at  $100^\circ\text{C}$  for 20 min during which a reverse bias of  $U_b = -9 \text{ V}$  was applied. b) DLTS spectra recorded for a diode,  $N_d^+(W)$  dependencies of which are shown in (a). The spectra are shifted along the vertical axis for clarity. Measurement parameters are given in the graph.

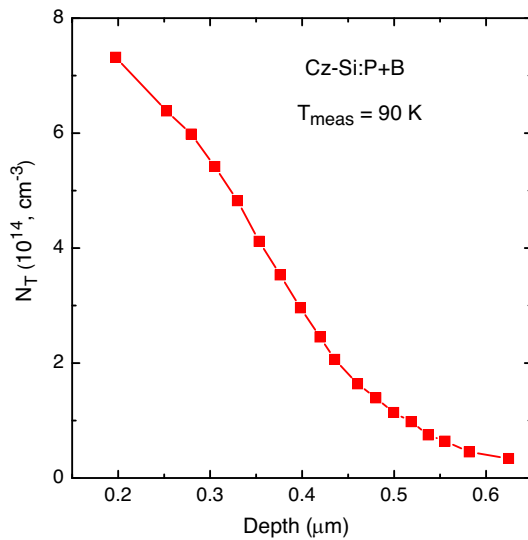


**Figure 6.** Concentration profile of the  $E_{0.175}$  trap,  $N_{E_{0.175}}(W)$ , in a diode on Cz-Si:P + B sample, which was subjected to the following subsequent treatments: 1) hydrogenation in H plasma at room temperature for 30 min; 2) annealing at  $100^\circ\text{C}$  for 20 min during which a reverse bias of  $U_b = -9 \text{ V}$  was applied. The profile measurements were conducted using L-DLTS with variable values of both bias and pulse voltages and the fixed difference of  $0.5 \text{ V}$  between  $U_b$  and  $U_p$  values. The “lambda” layer values have been taken into account upon calculations of the  $N_{E_{0.175}}$  and  $W$  values.<sup>[21]</sup>

Our interpretation of the results shown in Figure 2–9 will be briefly discussed in this section but a more detailed discussion can be found in Section 5. The RBA treatment at  $100^\circ\text{C}$  results in the appearance of mobile positively charged H atoms in the depletion region of the diodes. The  $\text{H}^+$  atoms interact with substitutional boron atoms and create the BH-related defect with the donor level at  $E_c - 0.175 \text{ eV}$ . The dissociation of the defect

responsible for the  $E_{0.175}$  trap upon annealing at  $290 \text{ K}$  occurs only after capture of an electron by the defect, and most likely this results in the appearance of separated substitutional boron and interstitial H atoms. The H atoms immediately capture available free electrons, become negatively charged, and interact with positively charged P atoms. The decrease in the  $N_d^+(W)$  values below the bulk value (curves 4–6 in Figure 7) can only be interpreted by the appearance of negatively charged H atoms and their passivation of electrical activity of phosphorus atoms.

Finally, it is found that a repetition of the RBA treatment on the diodes, which were previously subjected to an RBA–room temperature storage cycle, again results in the increase in the  $N_d^+(W)$  values and concentration of the  $E_{0.175}$  trap in the subsurface regions of the diodes, however, with reduced  $N_d^+(W)$  and  $N_{E_{0.175}}$  values compared with those induced by a previous RBA treatment, as a comparison of DLTS spectra 2 and 6 in Figure 9 shows. It is likely that this gradual reduction of the  $N_d^+(W)$  and  $N_{E_{0.175}}$  values upon the repeated RBA–room temperature storage cycles is mainly related to the electric-field stimulated drift of positively charged hydrogen atoms to the sample surface during the RBA treatments and with its permanent loss in the subsurface regions for 1) passivation of phosphorus donors and 2) RBA-induced reactions with the available boron atoms.

## 5. Discussion

The phenomena, which we have observed in the hydrogenated P + B co-doped Cz-Si samples, resemble those observed by Endrös et al. in hydrogenated carbon-rich Si samples.<sup>[47,48]</sup> Furthermore, the electronic properties of the  $E_{0.175}$  trap (DLTS signatures, electric field enhancement of electron emission rate, and thermal stability) detected by us are very close to those for the carbon–hydrogen defect observed by Endrös et al. Carbon

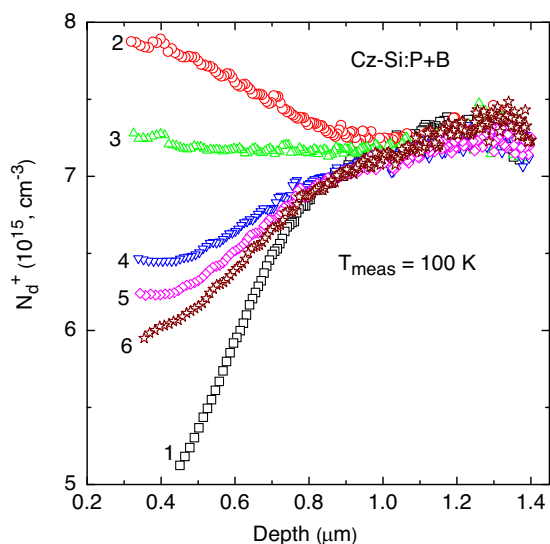


**Figure 7.** Spatial profiles of concentration of uncompensated ionized shallow donors measured at 100 K in a diode on Cz-Si:P+B sample, which was subjected to the following subsequent treatments: (1) hydrogenation in H plasma at room temperature for 30 min and annealing at 100 °C for 20 min under open circuit conditions; (2) annealing at 100 °C for 20 min during which a reverse bias of  $U_b = -9$  V was applied; (3)–(5) storage at 290 K for 40, 180, 300 min, respectively, under open circuit conditions; (6) storage at 300 K for 15 h under open circuit conditions.

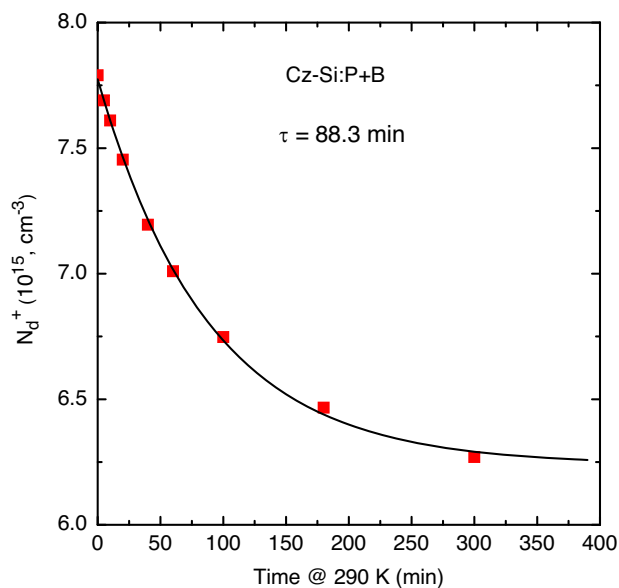


**Figure 8.** Decay of the average  $N_d^+(W)$  values in the range of 0.4–0.5  $\mu\text{m}$  from the surface for a hydrogenated and RBA-treated diode on Cz-Si:P+B sample upon keeping it at 290 K under open-circuit conditions. The solid line represents a monoexponential decay curve fitted to the experimental data.

concentration in the P + B co-doped samples used in our study is about  $4.5 \times 10^{16} \text{ cm}^{-3}$ , so the available carbon atoms might be responsible for the formation of the  $E_{0.175}$  trap and corresponding changes in the  $N_d^+(W)$  profiles. To probe this possibility,

we have subjected a few n-type Cz-Si samples with high carbon content ( $[C_s] \approx 4.0 \times 10^{17} \text{ cm}^{-3}$ ) to the treatments and measurements identical to those for the P + B co-doped samples. **Figure 10a** shows spatial profiles of uncompensated donors in a diode on a plasma-hydrogenated Si:P + C sample in an as-hydrogenated state and after annealing at 100 °C for 20 min, during which a reverse bias of  $U_b = -9$  V was applied. The RBA treatment has resulted in some increase in the  $N_d^+(W)$  values in the subsurface region of the diode; however, the increase is very much smaller than that in the P + B co-doped samples (Figure 6) and indicates that no additional donors have been created during the RBA. Figure 10b shows the conventional DLTS spectra for a diode on the Cz-Si:P + C material, the  $N_d^+(W)$  dependencies of which are shown in Figure 10a. Three dominant electron emission signals with their maxima at about 69, 78, and 90 K are observed in the DLTS spectrum of the plasma-hydrogenated sample. A comparison of DLTS signatures of the observed traps with those, which are available in the literature for silicon samples subjected to similar treatments, allows us to suggest that the peaks with their maxima at 69 and 78 K are related to acceptor levels of the C–O–H complexes,<sup>[43,44]</sup> and the peak with its maximum at 90 K to two C–H complexes.<sup>[32]</sup> The RBA treatment has resulted in some tiny changes in the magnitudes of the peaks due to the C–O–H complexes, and in a small increase in the magnitude of the peak due to the C–H complexes. A comparison of the results presented in Figure 5a,b with those in Figure 10a,b indicates that it is unlikely that substitutional carbon atoms are responsible for the appearance of the  $E_{0.175}$  trap in our P + B co-doped samples. We have further studied a range of hydrogenated n-type Cz-Si and FZ-Si samples, in which carbon concentration has not been specified, before and after the RBA treatments identical to those used in this work. In some of the samples, the RBA treatments resulted in the appearance of a DLTS signal with its maximum at a temperature close to that for the maximum of the  $E_{0.175}$  trap; however, concentrations of the corresponding traps never exceeded  $10^{13} \text{ cm}^{-3}$ . So, these findings indicate that the  $E_{0.175}$  trap and the RBA-induced changes in the  $N_d^+(W)$  values in the P + B co-doped samples are related to the presence of boron in these samples and its interactions with hydrogen atoms.

All the experimental results and calculations available in the literature indicate that the defect, which incorporates one boron and one hydrogen atom, is electrically neutral in crystalline silicon.<sup>[11–18,40,41]</sup> Our ab initio modeling results, which are presented earlier, are consistent with this statement. Taking into account those calculations, it is reasonable to suggest that the  $E_{0.175}$  trap and the RBA-induced changes in the  $N_d^+(W)$  dependencies in the P + B co-doped samples are related to the complex incorporating one boron and two hydrogen atoms,  $\text{BH}_2$ . The electronic properties of the  $E_{0.175}$  trap are consistent with those obtained for the  $\text{BH}_2$  defect by ab initio modeling and are similar to those of a carbon–hydrogen complex with donor properties, which was studied by Endrös et al.<sup>[47,48]</sup> and by Stübner et al.<sup>[32]</sup> It has been argued by Stübner et al. that the observed C–H donor complex ( $\text{CH}_B$  according to Stübner et al.<sup>[32]</sup>) incorporates more than one hydrogen atom, most likely two. It appears that the electronic properties of the  $\text{BH}_2$  and  $\text{CH}_B$  ( $\text{CH}_2$ ) complexes resemble those of a single bond-centered



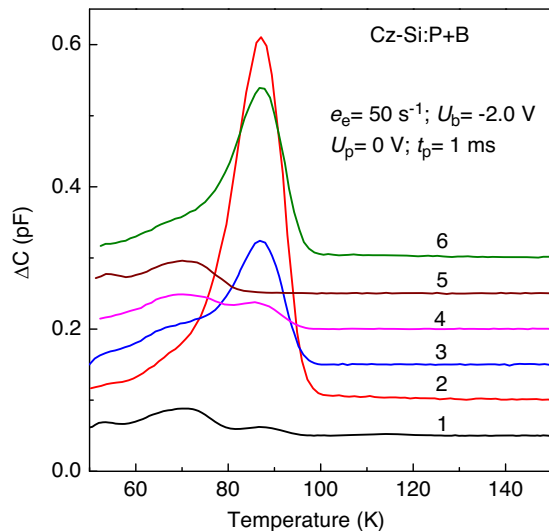


**Figure 9.** DLTS spectra recorded on a diode on Cz-Si:P+B sample, which was subjected to the following subsequent treatments: (1) hydrogenation in H plasma at room temperature for 30 min; (2) annealing at 100 °C for 20 min during which a reverse bias of  $U_b = -9$  V was applied; (3) and (4) storage at 290 K for 60 and 300 min, respectively, under open circuit conditions; (5) storage at 300 K for 15 h under open-circuit conditions; (6) annealing at 100 °C for 20 min with applied reverse bias of  $U_b = -9$  V. The spectra are shifted on Y axis for clarity. Measurement parameters are given in the graph.

hydrogen atom. All these defects possess a donor level at about 0.15–0.2 eV below the conduction band and are likely to be effective recombination centers in p-type Si samples.

In the light of our findings, we would like to consider the recent literature results on 1) the control of hydrogen content in solar Si materials by measurements of resistivity changes due to the formation of BH defects upon dark annealing of

hydrogenated boron-doped p-type Si crystals in the temperature range from 150 °C to about 300 °C,<sup>[9,10,49–51]</sup> and 2) LeTID occurring in p-type Si upon dark annealing in the same temperature range.<sup>[8,9,51–53]</sup> It should be noted that according to the recent studies,<sup>[9]</sup> the initial stages of the 1) and 2) processes occur with nearly identical time constants.

It is generally accepted that in Si samples hydrogenated by high-temperature ( $\geq 700$  °C) annealing in the presence of a hydrogen source with fast cooling down after the heat-treatment, majority of hydrogen exist in the form of hydrogen molecules at tetrahedral interstitial sites  $H_2(T)$ .<sup>[1,2,40,55–57]</sup> It was found by Pritchard et al. that in boron-doped Si crystals the  $H_2(T)$  dimers disappeared upon dark annealing of hydrogenated Si:B samples at temperatures exceeding 150 °C with simultaneous appearance of hydrogen–boron pairs.<sup>[55]</sup> The concentration of BH pairs has been monitored through the changes in magnitude of the infrared absorption line at  $1904\text{ cm}^{-1}$ .<sup>[54]</sup> The processes related to the transformation of the  $H_2(T)$  dimers to the HB pairs have been considered earlier in Pritchard et al.<sup>[55]</sup> and recently in Walter et al.<sup>[10,49]</sup> and Voronkov and Falster.<sup>[57]</sup> It has been argued in the recent studies that the first step in these processes is the dissociation of the  $H_2(T)$  molecule to two H atoms, which became positively charged in p-type Si. Furthermore, these  $H^+$  atoms interact with negatively charged boron atoms according to the Reaction (R1), resulting in the appearance of two neutral BH pairs. It has been further suggested that the possible direct interaction of  $H_2(T)$  molecules with a boron atom is not a dominant reaction, but when occurring it results in the appearance of a BH pair and a separated hydrogen atom.<sup>[56]</sup> On the contrary, it was argued in the earlier study that the direct interaction of  $H_2$  molecule with the  $B_s$  atoms occurs, and there is a barrier of about 0.8 eV for the separation of a hydrogen atom from the BH pair.<sup>[55]</sup>

The elimination kinetics of the  $H_2(T)$  dimers upon heat-treatment of hydrogenated n-type Cz-Si crystals at 300 °C has been reported in Murin et al.<sup>[58]</sup> It has been found that about

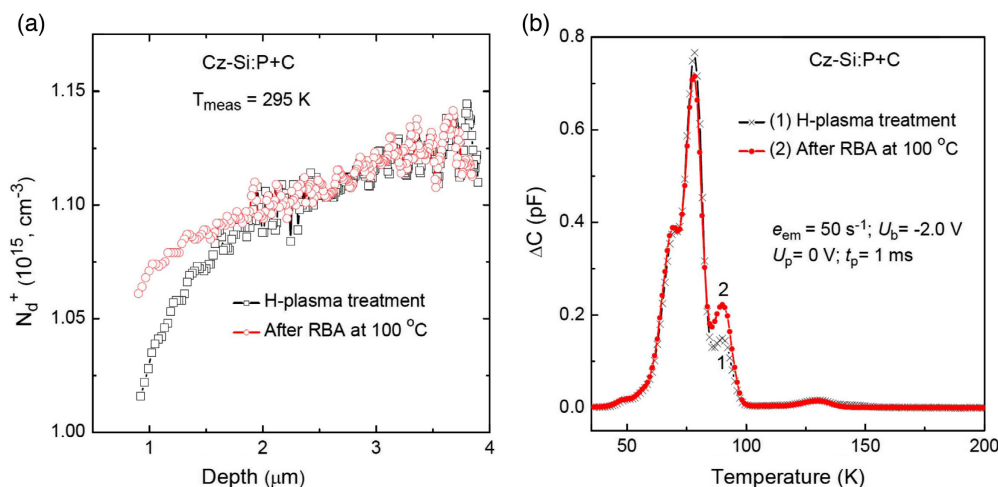


**Figure 10.** a) Spatial profiles of concentration of uncompensated shallow donors measured at 295 K in a diode on Cz-Si:P+C sample, which was subjected to the following subsequent treatments: (1) hydrogenation in H plasma at room temperature for 30 min; (2) annealing at 100 °C for 20 min during which a reverse bias of  $U_b = -9$  V was applied. b) DLTS spectra recorded for a diode,  $N_d^+(W)$  dependencies of which are shown in (a). Measurement parameters are given in the graph.

50% of the dimers survive after annealing at 300 °C for 120 min. This result is not consistent with the direct dissociation of  $H_2(T)$  molecules in the temperature range close to 200 °C as suggested in Voronkov and Falster.<sup>[57]</sup> On the contrary, it is known that the  $H_2(T)$  molecules are mobile in Si at temperatures slightly above 300 K, and their diffusion coefficient in  $cm^2 s^{-1}$  has been determined as  $D(H_2) = 2.6 \times 10^4 \times \exp\{-(0.78 \pm 0.05 \text{ eV})/kT\}$ .<sup>[56]</sup> Taking into account the aforementioned findings, we support the suggestion put forward in Pritchard et al.,<sup>[55]</sup> according to which the direct interaction of mobile  $H_2(T)$  molecules with substitutional boron atoms is the dominant reaction that occurs during the initial stages of 150–250 °C thermal treatments of p-type Si crystals hydrogenated at high temperatures (either by firing or heat-treatments in a  $H_2$  gas ambient).

We can now go further and suggest a possible sequence of defect reactions related to LeTID occurring in p-type solar Si upon dark annealing in the temperature range 150–250 °C. The first reaction of the sequence is the direct interaction of mobile  $H_2$  molecules with substitutional boron atoms that results in the formation of the  $BH_2$  defects. The  $H_2$  molecules are created upon fast firing process in the samples covered with hydrogen-rich dielectric layers, particularly,  $SiN_x:H$ . The  $BH_2$  defects are positively charged in p-type Si, and therefore are effective traps for electrons, so their formation results in the decrease in lifetime of minority carriers (electrons), and in the decrease in samples resistivity as the appearance of one  $BH_2$  defect is accompanied by the removal of two holes. Further annealing results in the separation of one hydrogen atom from the  $BH_2$  complex, and subsequent capture of this separated atom by another boron atom with the formation of two neutral BH pairs (reverse of Reaction (R5) with an energy gain of 0.34 eV). This process results in the regeneration of the degraded lifetime and the growth of infrared absorption line at  $1904 \text{ cm}^{-1}$ . It should be noted that the  $BH_2^+ + B_s^- \rightarrow 2BH^0$  reaction does not result in resistivity changes in p-type Si. The binding energy of the BH pair is not high (0.73 eV according to our calculations, Reaction (R1)), so the prolonged annealing of the hydrogenated B-doped Si results in the dissociation of the pairs and interactions of hydrogen atoms with other sinks, which include grain boundaries and the sample surface.

## 6. Conclusions

We have revisited the structure, binding energies, and electronic properties of boron–hydrogen defects in silicon using modern density functional methods. We confirm previous structures for BH and  $BH_2$  complexes as stable with respect to dissolved boron and hydrogen (either in atomic and molecular forms). However, we find that  $BH_2$  is unstable against formation of BH pairs. We also confirm that H effectively deactivates the electronic activity of boron upon formation of the BH and  $BH_2$  defects. **The  $BH_2$  defect is predicted to have a donor level at  $E_c - E(0/+) = 0.24 \text{ eV}$ .**

We also compared the magnitude of the capture radius for the reaction between bond-centered hydrogen and BH-complexes with the analogous quantities for other probable H-traps, namely, substitutional carbon and substitutional boron ions. It is found that despite being a neutral defect, the permanent and orientable

electric dipole and strain fields make the BH pair an effective trap for mobile H atoms. At least, it is as efficient as substitutional carbon.

Experimentally, an effective formation of an electron trap with activation energy of  $\approx 0.175 \text{ eV}$  relative to the conduction band edge is detected in the hydrogenated Si:P + B samples after RBA treatments at 100 °C. The trap is a donor with electronic properties close to those predicted by ab initio calculations for the boron–dihydrogen complex. It is argued that the trap is related to the  $BH_2$  defect. The donor character of  $BH_2$  suggests that it can be a very efficient recombination center of minority carriers in B-doped p-type Si crystals.

We finally propose a sequence of defect reactions, which result in the resistivity and minority carrier lifetime changes (LeTID) of hydrogenated p-type solar Si:B crystals, upon dark annealing in the temperature range 150–250 °C.

## Acknowledgements

The authors would like to thank EPSRC (UK) for funding this work via grant EP/T025131/1. J.A.T.D.G. would like to thank the Government of the Philippines through the Department of Science and Technology (DOST) for her Ph.D. funding. J.C. thanks the support of the i3N projects, Refs. UIDB/50025/2020 and UIDP/50025/2020, financed by the Fundação para a Ciência e a Tecnologia in Portugal.

## Conflict of Interest

The authors declare no conflict of interest.

## Data Availability Statement

Research data are not shared.

## Keywords

ab initio modeling, boron–hydrogen, DLTS, LeTID, passivation, silicon, solar cells

Received: June 27, 2021

Revised: September 4, 2021

Published online: September 17, 2021

- [1] S. H. Lee, M. F. Bhopal, D. W. Lee, S. H. Lee, *Mater. Sci. Semicond. Processing* **2018**, 79, 66.
- [2] B. J. Hallam, P. G. Hamer, A. C. Ciesla née Wenham, C. E. Chan, B. V. Stefani, S. Wenham, *Prog. Photovolt. Res. Appl.* **2020**, 28, 1217.
- [3] J. Mullins, S. Leonard, V. P. Markevich, I. D. Hawkins, P. Santos, J. Coutinho, A. C. Marinopoulos, J. D. Murphy, M. P. Halsall, A. R. Peaker, *Phys. Status Solidi A* **2017**, 214, 1700304.
- [4] H. C. Sio, S. P. Phang, H. T. Nguyen, Z. Hameiri, D. Macdonald, *Prog. Photovolt. Res. Appl.* **2020**, 28, 493.
- [5] J. A. T. de Guzman, V. P. Markevich, D. Hiller, I. D. Hawkins, M. P. Halsall, A. R. Peaker, *J. Phys. D: Appl. Phys.* **2021**, 54, 275105.
- [6] W. Kwapil, J. Schon, T. Niewelt, M. C. Schubert, *IEEE J. Photovolt.* **2020**, 10, 1591.

- [7] D. Chen, P. Hamer, M. Kim, C. Chan, A. Ciesla nee Wenham, F. Rougieux, Y. Zhang, M. Abbott, B. Hallam, *Sol. Energy Mater. Sol. Cells* **2020**, 207, 110353.
- [8] D. Chen, M. Vaqueiro Contreras, A. Ciesla, P. Hamer, B. Hallam, M. Abbott, C. Chan, *Progr. Photovolt. Res. Appl.* **2020**, <https://doi.org/10.1002/ppp.3362>.
- [9] B. Hammann, L. Rachdi, W. Kwapił, F. Schindler, M. C. Schubert, *Phys. Status Solidi RRL* **2021**, 15, 2000584.
- [10] D. C. Walter, D. Bredemeier, R. Falster, V. V. Voronkov, J. Schmidt, in *Proc. 37th Eur. Photovoltaics Sol. Energy Conf. Exhib.*, WIP, Munich, Germany **2020**, pp. 140–144.
- [11] C.-T. Sah, J. Y.-C. Sun, J. J.-T. Tzou, *Appl. Phys. Lett.* **1983**, 43, 204.
- [12] J. I. Pankove, D. E. Carlson, J. E. Berkeyheiser, R. O. Wance, *Phys. Rev. Lett.* **1983**, 51, 2224.
- [13] J. I. Pankove, P. J. Zanzucchi, C. W. Magee, G. Lucovsky, *Appl. Phys. Lett.* **1985**, 46, 421.
- [14] N. M. Johnson, *Phys. Rev. B* **1985**, 31, 5525.
- [15] M. Stutzmann, *Phys. Rev. B* **1987**, 35, 5921.
- [16] K. J. Chang, D. J. Chadi, *Phys. Rev. Lett.* **1998**, 60, 1422.
- [17] P. J. H. Denteneer, C. G. Van de Walle, S. T. Pantelides, *Phys. Rev. B* **1989**, 39, 10809.
- [18] L. Korpas, J. W. Corbett, S. K. Estreicher, *Phys. Rev. B* **1992**, 46, 12365.
- [19] J. T. Borenstein, J. W. Corbett, S. J. Pearton, *J. Appl. Phys.* **1993**, 73, 2751.
- [20] B. Pajot, B. Clerjaud, *Optical Absorption of Impurities and Defects in Semiconducting Crystals: Electronic Absorption of Deep Centers and Vibrational Spectra*, Springer-Verlag, New York **2013**.
- [21] A. R. Peaker, V. P. Markevich, J. Coutinho, *J. Appl. Phys.* **2018**, 123, 161559.
- [22] L. Dobczewski, A. R. Peaker, K. Bonde Nielsen, *J. Appl. Phys.* **2004**, 96, 4689.
- [23] J. Heyd, G. E. Scuseria, M. Ernzerhof, *J. Chem. Phys.* **2003**, 118, 8207.
- [24] J. Heyd, G. E. Scuseria, M. Ernzerhof, *J. Chem. Phys.* **2006**, 124, 219906.
- [25] G. Kresse, J. Furthmüller, *Phys. Rev. B* **1996**, 54, 11169.
- [26] G. Kresse, J. Furthmüller, *Comput. Mater. Sci.* **1996**, 6, 15.
- [27] P. E. Blöchl, *Phys. Rev. B* **1994**, 50, 17953.
- [28] J. P. Perdew, K. Burke, M. Ernzerhof, *Phys. Rev. Lett.* **1996**, 77, 3865.
- [29] C. Freysoldt, J. Neugebauer, C. G. Van de Walle, *Phys. Rev. Lett.* **2009**, 102, 016402.
- [30] K. Bonde Nielsen, B. Bech Nielsen, J. Hansen, E. Andersen, J. U. Andersen, *Phys. Rev. B* **1999**, 60, 1716.
- [31] Y. Kamiura, M. Tsutsue, Y. Yamashita, F. Hashimoto, *J. Appl. Phys.* **1995**, 78, 4478.
- [32] R. Stübner, V. Kolkovsky, J. Weber, *J. Appl. Phys.* **2015**, 118, 055704.
- [33] R. Stübner, V. Kolkovsky, J. Weber, N. V. Abrosimov, C. M. Stanley, D. J. Backluns, S. K. Estreicher, *J. Appl. Phys.* **2020**, 127, 045701.
- [34] D. J. Bacon, D. M. Barnett, R. O. Scattergood, *Prog. Mat. Sci.* **1980**, 23, 51.
- [35] S. L. Dudarev, P.-W. Ma, *Phys. Rev. Mat.* **2018**, 2, 033602.
- [36] A. George, in *Properties of Crystalline Silicon*, EMIS Datareviews Series No. 20 (Ed.: R. Hull), INSPEC, London, UK **1999**.
- [37] E. Clouet, C. Varvenne, T. Jourdan, *Comp. Mat. Sci.* **2018**, 147, 49.
- [38] L. Bengtsson, *Phys. Rev. B* **1999**, 59, 12301.
- [39] G. Makov, M. C. Payne, *Phys. Rev. B* **1995**, 51, 4014.
- [40] A. R. Peaker, V. P. Markevich, L. Dobaczewski, in *Defects in Microelectronic Materials and Devices* (Eds.: D. M. Fleetwood, S. T. Pantelides, R. D. Schrimpf), CRC Press, Boca Raton, FL **2009**.
- [41] M. Stavola, in *Properties of Crystalline Silicon*, EMIS Datareviews Series No. 20 (Ed.: R. Hull), INSPEC, London, UK **1999**.
- [42] L. C. Kimerling, J. L. Benton, *Appl. Phys. Lett.* **1981**, 39, 410.
- [43] M. Vaqueiro-Contreras, V. P. Markevich, M. P. Halsall, A. R. Peaker, P. Santos, J. Coutinho, S. Öberg, L. I. Murin, R. Falster, J. Binns, E. V. Monakhov, B. G. Svensson, *Phys. Status Solidi RRL* **2017**, 11, 1700133.
- [44] M. Vaqueiro-Contreras, V. P. Markevich, J. Mullins, M. P. Halsall, L. I. Murin, R. Falster, J. Binns, J. Coutinho, A. R. Peaker, *J. Appl. Phys.* **2018**, 123, 161415.
- [45] J. L. Hartke, *J. Appl. Phys.* **1968**, 39, 4871.
- [46] B. Sopori, Y. Zhang, N. M. Ravindra, *J. Electron. Mater.* **2001**, 30, 1616.
- [47] A. Endrös, *Phys. Rev. Lett.* **1989**, 63, 70.
- [48] A. L. Endrös, W. Krüchler, F. Koch, *J. Appl. Phys.* **1992**, 72, 2264.
- [49] D. C. Walter, D. Bredemeier, R. Falster, V. V. Voronkov, J. Schmidt, *Sol. Energy Mater. Sol. Cells* **2019**, 200, 109970.
- [50] A. Herguth, C. Winter, *IEEE J. Photovolt.*, <https://doi.org/10.1109/JPHOTOV.2021.3074463>.
- [51] C. Winter, J. Simon, A. Herguth, *Phys. Status Solidi A*, <https://doi.org/10.1002/PSSA.202100220>.
- [52] D. Chen, M. Kim, B. V. Stefani, B. J. Hallam, M. D. Abbott, C. E. Chan, R. Chen, D. N. R. Payne, N. Nampalli, A. Ciesla, T. H. Fung, K. Kim, S. R. Wenham, *Sol. Energy Mater. Sol. Cells* **2017**, 172, 293.
- [53] T. Luka, M. Turek, C. Hagendorf, *Sol. Energy Mater. Sol. Cells* **2018**, 187, 194.
- [54] C. Chan, T. H. Fung, M. Abbott, D. Payne, A. Wenham, B. Hallam, R. Chen, S. Wenham, *Sol. RRL* **2017**, 1, 1600028.
- [55] R. E. Pritchard, J. H. Tucker, R. C. Newman, E. C. Lightowers, *Semicond. Sci. Tech.* **1999**, 14, 77.
- [56] V. P. Markevich, M. Suezawa, *J. Appl. Phys.* **1998**, 83, 2988.
- [57] V. V. Voronkov, R. Falster, *Phys. Status Solidi B* **2017**, 254, 1600779.
- [58] L. I. Murin, V. P. Markevich, M. Suezawa, J. L. Lindstrom, M. Kleverman, T. Hallberg, *Physica B* **2001**, 302–303, 180.